10/10/2015

DZHELEPOV LABORATORY OF NUCLEAR PROBLEMS

CALIBRATION PROCEDURE OF HYBRID PIXEL DETECTORS WITH CHROMIUM DOPED GALLIUM ARSENIDE SENSOR AND TIMEPIX READOUT CHIP

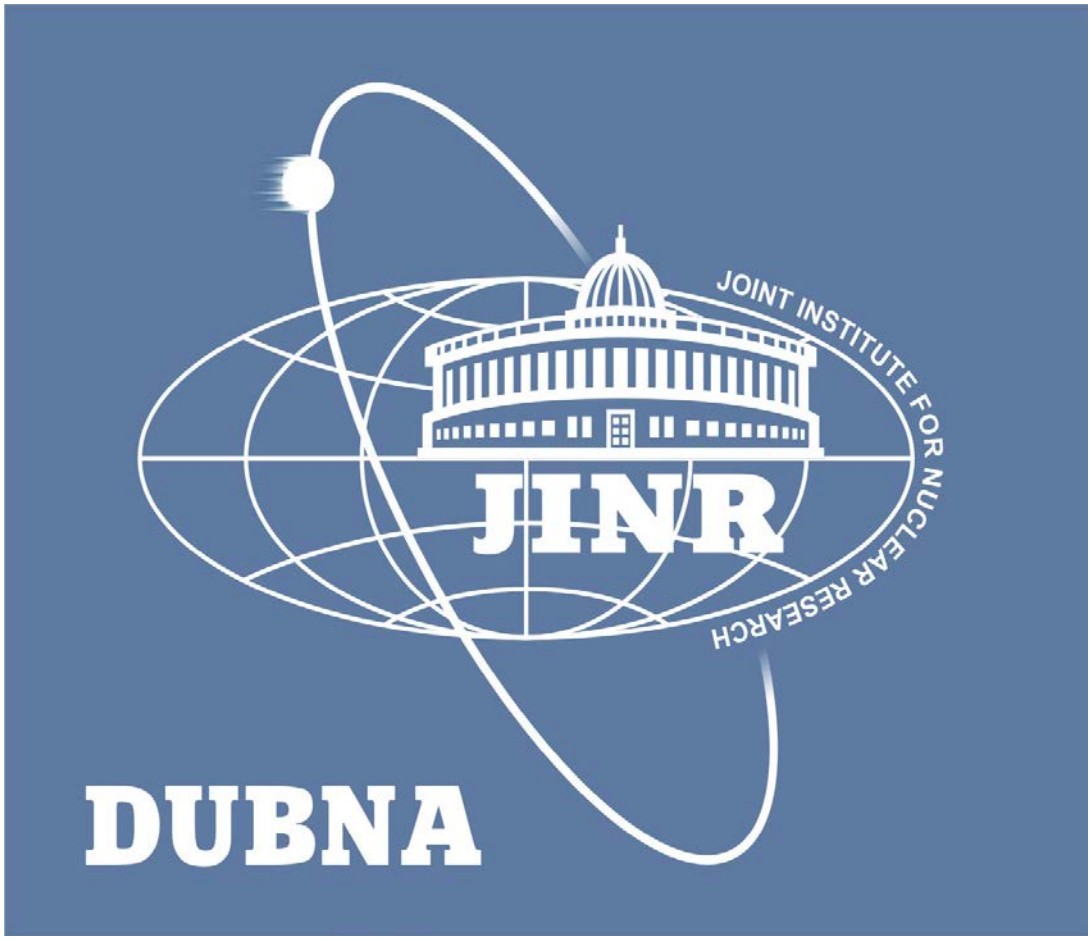

Supervisor: Prof. G. Shelkov | Student: Ibrahim Hany

Abstract

The Medipix/Timepix detectors were developed by collaboration at CERN, such development started since the 1990s, from that time; it has been going through many improvements, and many versions of the hybrid pixel detector were produced. One of the newest versions is Timepix readout chip, it has many advantages compared to its predecessors, namely in its three operation modes. Conventionally the sensor for such chips is made from silicon. Silicon is replaced by GaAs:Cr due to its higher X-Ray absorption efficiency especially at high energies (above 20 KeVs). In our work we studied the energy calibration for such detector operating on the ToT mode.

Table of Contents

Introduction

Hybrid pixel detectors are used in various fields of physics experiments and applications. In recent years they had shown great impact in the field of biology and geology. In high energy physics these detectors are used for the registration of particles, and especially in tracking and timing application. Si has been used as a sensor material in such detectors, however it has some disadvantages due to its relatively low attenuation coefficient for X-Ray, a disadvantage that paved the road for other sensor materials like GaAs:Cr and CdTe.

In this report, we start from the basic physical principles of semiconductor detectors, and end by the energy calibration curve of a cutoff technology hybrid pixel semiconductor detector. Our main work is performing the iterative procedure of per pixel energy calibration of hybrid pixel detectors using GaAs:Cr as a sensor material.

Literature review

Theory

Basic principle of semiconductor detectors

When a charged particle passes through a semiconductor with the band structure shown in Figure 1, the overall significant effect is the production of many electron-hole pairs along the track of the particle. The production process may be either direct or indirect, in that the particle produces high-energy electrons (or delta rays) that subsequently lose their energy in producing more electron-hole pairs. Regardless of the detailed mechanisms involved, the quantity of practical interest for detector applications is the average energy expended by the primary charged particle to produce one electron-hole pair. This quantity, often loosely called the ionization energy and given the symbol E, is experimentally observed to be largely independent of the energy of the incident radiation. This important simplification allows interpretation of the number of electron-hole pairs produced in terms of the incident energy of the radiation, provided the particle is fully stopped within the active volume of the detector.

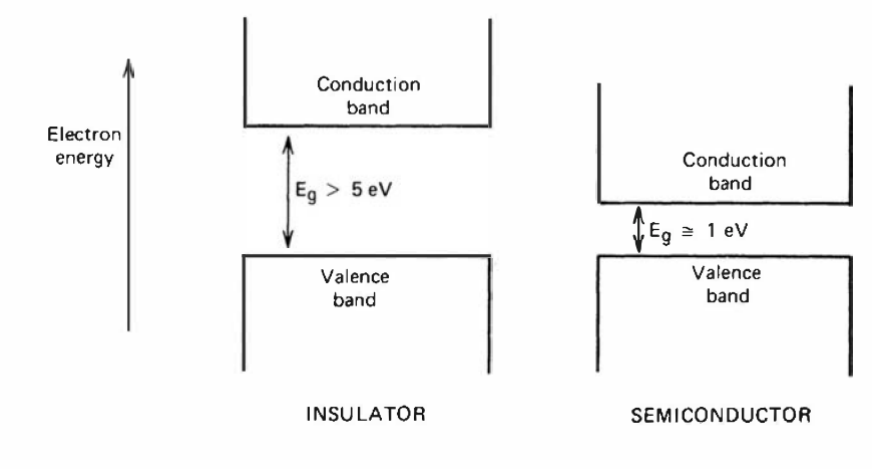

Figure 1: Band structure for electron energies in insulators and semiconductors. (Knoll, 2010)

When radiation interacts in a semiconductor, the energy deposition always leads to the creation of equal numbers of holes and electrons. This statement holds regardless of whether the host semiconductor is pure or intrinsic, or doped as p-type or n-type. Just as equal numbers of free electrons and positive ions are created in a gas, every conduction electron produced in a semiconductor must also create a hole in the valence band, leading to an exact balance in the initial number of created charges. It should also be emphasized that the doping levels typical in p- or n-type semiconductors are so low that these atoms play no significant role in determining the nature of the radiation interactions in the material. Thus p-type or n-type silicon of equal thickness will present identical interaction probabilities for gamma rays, and the range of charge particles in either type will also be the same.

The dominant advantage of semiconductor detectors lies in the smallness of the ionization energy. The value of "E" for either silicon or germanium is about 3 eV, compared with about 30

eV required to create an ion pair in typical gas-filled detectors. Thus, the number of charge carriers is 10 times greater for the semiconductor case, for a given energy deposited in the detector. The increased number of charge carriers has two beneficial effects on the attainable energy resolution. The statistical fluctuation in the number of carriers per pulse becomes a smaller fraction of the total as the number is increased. This factor often is predominant in determining the limiting energy resolution of a detector for medium to high radiation energy. At low energies, the resolution may be limited by electronic noise in the preamplifier, and the greater amount of charge per pulse leads to a better signal/noise ratio.

More detailed examination shows that E depends on the nature of the incident radiation.

Most (ordinary) detector calibrations are carried out using alpha particles. All experimental values obtained using other light ions or fast electrons seem to be fairly close, but differences as large as 2.2 % have been reported between proton and alpha particle excitation in silicon. These observed differences point up the need to carry out detector calibration using a radiation type that is identical to that involved in the measurement itself if precise energy values are required.

The ionization energy is also temperature dependent. For the most significant detector materials, the value of E increases with decreasing temperature. E in silicon is about 3% greater at liquid nitrogen temperature compared with room temperature. There is also evidence that the ionization energy can be dependent on the energy of the radiation, especially in the soft X-ray energy range. (Knoll, 2010)

Basic Principle of pixel detectors

Detectors in which the position of interaction of the incident radiation is sensed together with its energy have application in a number of different areas. The two major types of detectors used for position sensing for charged particles are gas-filled devices and silicon or germanium semiconductor diode detectors. The latter types are sometimes preferred because of their compactness and low bias voltage compared with gas-filled detectors.

Semiconductor detectors, because of their greater stopping power, are also better suited for applications involving long-range radiations.

The "brute force" approach to obtaining two-dimensional position information from a single-sided silicon detector is to fabricate the top electrode as a checkerboard pattern of individual small elements that are electrically isolated from each other. When the dimensions of the individual electrodes are a millimeter or larger, this type of device is usually called a pad detector. For electrode dimensions smaller than one millimeter, the common terminology is pixel detector. Electrical connection must be made to each individual electrode and separate electronic readout channels provided for each.

One advantage of this approach is that the small size of each individual electrode results in a relatively small capacitance and leakage current, and thus the electronic noise is

reduced considerably from that observed from microstrip detectors of equivalent dimensions.

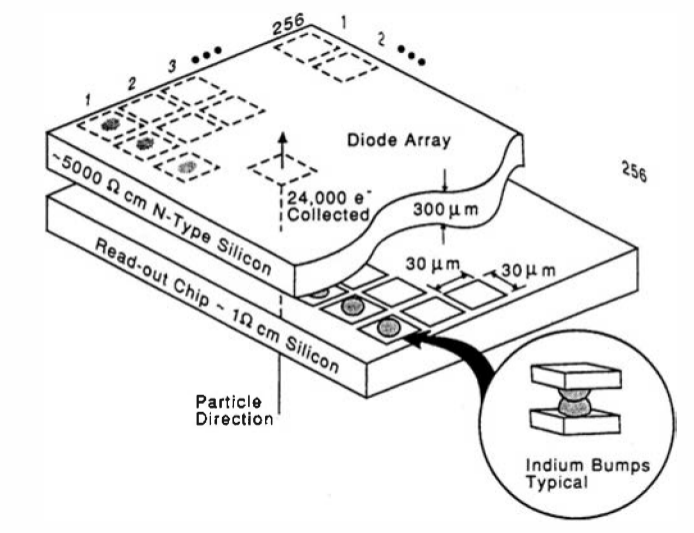

Figure 2: A hybrid pixel detector consisting of separate detector and electronics chips connected through indium bump bonds. (Knoll, 2010)

In addition to resulting in a lower noise level, the lower leakage current may permit room temperature operation when devices with larger electrode dimensions may require cooling.

Providing separate electrical contacts to each pixel presents a significant challenge. For small-area detectors in which the pixels or pads are sufficiently large, wire bonding techniques can be used to provide electrical connection from each pixel to the edge of the wafer. Alternatively, some double metal layer constructions allow contact to the interior pixels. (Knoll, 2010)

However, in the more common approach, illustrated in Figure 2 (Knoll, 2010) , a pixel detector chip is connected to a separate readout chip using flip chip solder bonding, or indium bump bonds.

The readout chip is fabricated with exactly the same pitch as the detector pixels, so each bump provides an electrical connection between a single pixel and its corresponding readout electronics.

It is tempting to think about integrating the detector and readout electronics in a monolithic structure on a single silicon chip. Progress in this direction has been inhibited by several problems, including the basic incompatibility between the high-resistivity silicon needed for substantial depletion regions for the detector and the lower resistivity silicon common in the fabrication of integrated circuits (ICs). There are also conflicts between the high-temperature processes typical of ICs and the lower temperatures needed to preserve

carrier lifetimes in the detector, and between the high voltages required for detector depletion and the lower voltages characteristic of IC operation.

Although there is continuing interest and effort to carry out this monolithic integration of the detector and electronics, present pixel or pad detectors are more often based on separate structures for each.

Pixel or pad detectors typically have active areas that are limited to a few square centimeters. Larger detector areas can be achieved by assembling individual modules into arrays, although at the expense of increasing complexity in what is already a complex device. (Knoll, 2010)

Medipix/Timepix

CERN Collaboration

Medipix is a family of photon counting and particle tracking pixel detectors developed by an international collaboration, hosted by CERN. Medipix 2 and Medipix 3 are collaborations between number of European Universities and Research Institutes. The aim of the Collaboration is to carry out the design and evaluation of the semiconductor pixel detectors called Medipix (or newly Timepix). The hybrid silicon pixel detector device Medipix was designed for imaging by single quantum counting in each pixel. The device consists of a pixelated sensor chip and a read-out chip containing the amplifier, discriminators and counter(s) for each pixel.

The Timepix chip uses an external clock with a frequency of up to 100 MHz as a time reference. Each pixel contains a preamplifier, a discriminator with hysteresis and 4-bit DAC for threshold adjustment, synchronization logic and a 14-bit counter with overflow control. Moreover, each pixel can be independently configured in one of four different modes: masked mode: pixel is off, counting mode: 1-count for each signal over threshold, TOT mode: the counter is incremented continuously as long as the signal is above threshold, and arrival time mode: the counter is incremented continuously from the time the first hit arrives until the end of the shutter. The chip resembles very much the Medipix2 chip physically and can be readout using slightly modified versions of the various existing systems.

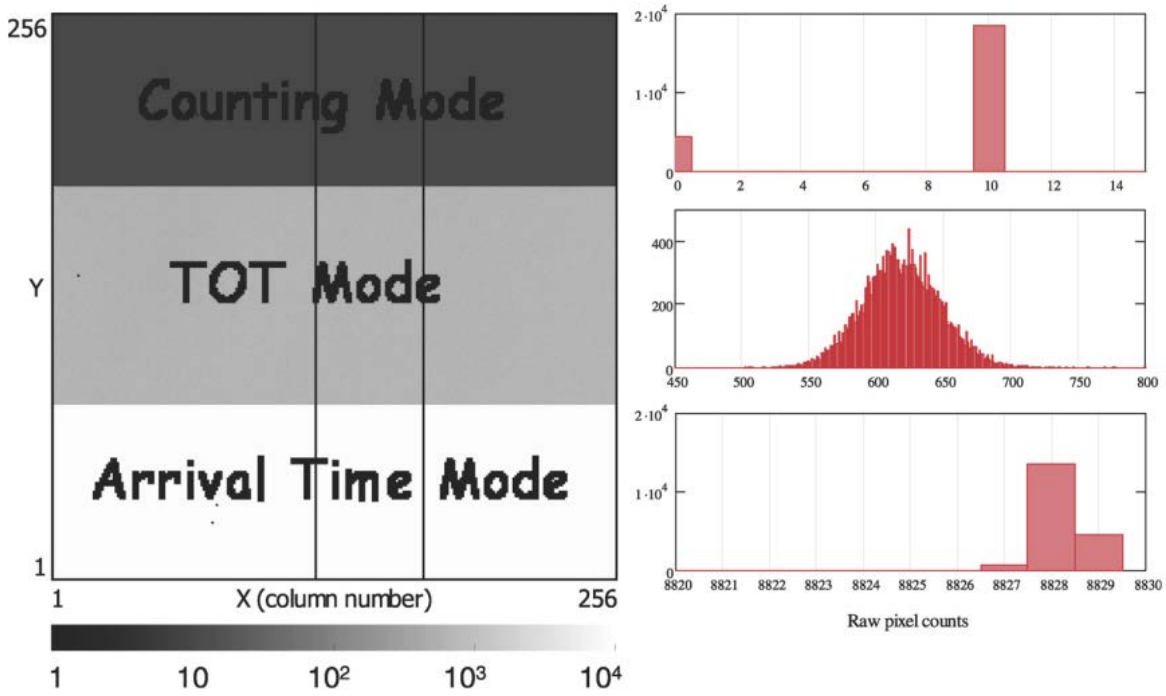

Figure 3: On the left is a full matrix 2D image response of an equalized chip after sending 10 test pulses of approximately 2.3 Ke^-. The matrix is split into three different working modes and the pixels that form the names are masked. On the right the histogram for each area (operation mode) is shown. The operating frequency is set to approximately 50 MHz. (Llopart, Ballabriga, Campbell, Tlustos & Wong, 2007)

The Timepix chip has been designed using a commercial 0.25 µm technology, with a pixel cell of 55x55 µm ^{2} .Each pixel can be programmed independently in counting, energy or arrival time modes. The chip has been characterized using an external test pulse. Initial measurements show an electronic pixel noise of ~100 e^- rms and a full matrix threshold variation ~35 e^- rms after equalization. The minimum detectable charge is ~650 e^- . In TOT mode the energy resolution (ΔTOT/TOT) is better than 5% if the input charge is ≥ 1 ke^- above threshold. The measured time-walk per pixel is ≤50 ns. (Llopart, Ballabriga, Campbell, Tlustos & Wong, 2007)

JINR improvements

Silicon is the standard semiconductor sensor material for pixelated detectors of Medipix type. Due to its homogeneity and stability it provides a high detector and image quality. However, because of its low Z number, Si has a low X-ray absorption efficiency at energies above 20 keV and is therefore not optimal as sensor material for medical imaging and non-destructive high Z material analysis. The compound semiconductor sensor materials GaAs (31, 33) and CdTe (48, 52) have a higher Z than Si (14) and therefore a better X-ray absorption efficiency. The recent progress in growing and processing of these materials improved detector quality and make them interesting as efficient sensor material for X-ray imaging applications. For investigations on these sensor materials they are bump bonded to Timepix/Medipix readout chips. The gallium arsenide doped by chromium (GaAs:Cr) is a new promising material developed at the Tomsk State University. The GaAs sensors were produced by means of the Liquid Encapsulated Czochralski method (LEC). The initial LEC GaAs material is doped by a shallow donor Sn or Te.

Then the layers of electronic conductivity type of the material are compensated by a deep acceptor Cr by means of controlled diffusion at high temperature. This results in a semi-insulating GaAs material with a high resistivity and a high value of an electron diffusion length (in comparison with LEC GaAs).

Figure 4: The hybrid pixel detector Timepix with USB interface FITPix

First in the world assembly of the Timepix ASIC and GaAs:Cr sensor made for JINR Laboratory of Nuclear Problem is shown on Figure 4. One can see two of the three main parts of which a Timepix assembly always consists of: the sensor layer and the Timepix ASIC (Figure 5). The readout interface (e.g. USB-readout FITPix) is necessary to extract the data from the ASIC and transmit it to the PC.

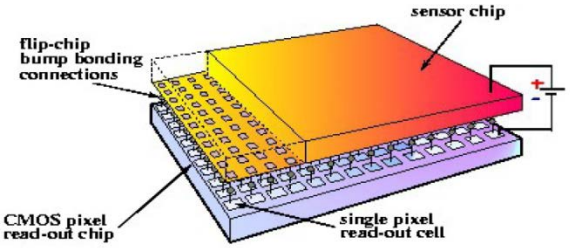

Figure 5: The structure of the Timepix detector

The semiconductor sensor layer (silicon Si, cadmium telluride CdTe and gallium arsenide GaAs) is the part of the detector. The size of the sensor material is usually about 1.4 cm x 1.4 cm and it is 0.3 mm - 1 mm thick. Particles which are passing the sensor material are scattered and deposit their energy within the sensor layer. By extracting this energy from the sensor we can make the particle tracks "visible". The ASIC has two main purposes: on the one hand it is needed to extract the deposited energy information out of the sensor and on the other hand together with the electrodes on the sensor backside it provides the pixelation of the sensor layer. The pixel grid on the ASIC is connected to the sensor layer by the bump-bonds. One pixel on the ASIC is quadratic and has a side length of 55 μm. In investigated detector the pixel pitch is 55 μm. But chips with 110 μm and 220 μm pixel pitch are available as well. The dimension of pixel matrix is 256 x 256 (for 55 μm pitch).

Application

Pixel detectors

Pixel detectors have been originally developed for particle physics applications. The next generation of experiments at hadron colliders can greatly profit from the unique characteristics of the pixel detectors provided these can be tailored to the demanding environment expected at these machines. These requirements boosted the activity around pixel detectors and also favored their development for imaging applications in biomedicine and in astronomy.

The driving projects for the next generation of pixel detectors are the experiments at the Large Hadron Collider (LHC). Three of the four large area pixel detectors currently in construction will constitute the innermost layers of three LHC experiments: ATLAS, CMS and ALICE. The fourth pixel detector is also designed for a hadron collider, Fermi lab's Tevatron, in the BTeV experiment. This is no surprise as pixel detectors can efficiently cope with the high particle densities and the large integral particle fluxes, both generated close to the interaction region of high luminosity as accelerators.

The development of hybrid pixel detectors for particle detection with high spatial resolution in high energy physics experiments has spun off a number of developments with applications in imaging, most notably biomedical imaging, but also imaging in X-ray astronomy. In the latter, the reconstruction of low energy X-ray images originating from astronomical point sources with high spatial and high energy resolution at moderate data rates is the challenge. So far this goal has been met best by using fully depleted pn-CCD detectors. For the next generation of X-ray satellites, however, semi-monolithic pixel devices with excellent spectroscopic performance are in the focus of development. The largest progress has been achieved in recent years in the development of pixel detectors or x-ray imaging or applications in radiology and in protein crystallography using synchrotron radiation X-rays. Another field in which pixel detector developments have created new possibilities for real-time imaging is that of-biomedical autoradiography, where most commonly low energy β radiation from radio-labeled tissue must be detected with high spatial resolution and high efficiency. Also γ emitters are occasionally considered. The use and development of pixel detectors in medical or astrophysical imaging systems like Compton cameras is also addressed by various research groups. (Rossi, Fischer, Rohe, Wermes, 2005)

MediPix/TimePix

The main application of hybrid pixel detectors with single photon counting mode in biomedical research is obtaining of X-ray images of high resolution and high contrast (detectors at synchrotron radiation sources, research microtomography), roentgenography and tomography of materials with small density variations (radiography of soft biological tissues, angiography and mammography). However, a new property of these detectors, namely the ability to measure the photon energy is promising for the development of new methods of X-ray diagnostics, because it allows the identification of the elemental composition of the studied biological objects.

Using the new detectors is of interest for geophysical surveys, as the increase of mineral resource base is currently associated not only with the search for new mineral deposits, but also

with the revaluation of reserves, with preparations for the development of reserve deposits, with involvement in the mining of mineral poor deposits and unconventional raw materials, previously considered unpromising, with the development of new environmentally friendly schemes of complex technological processing of raw materials and waste disposal to ensure recovery of all useful components with minimal losses, with the rational management of natural resources.

Energy Calibration

In this section we illustrate in some detail the procedure of our project.

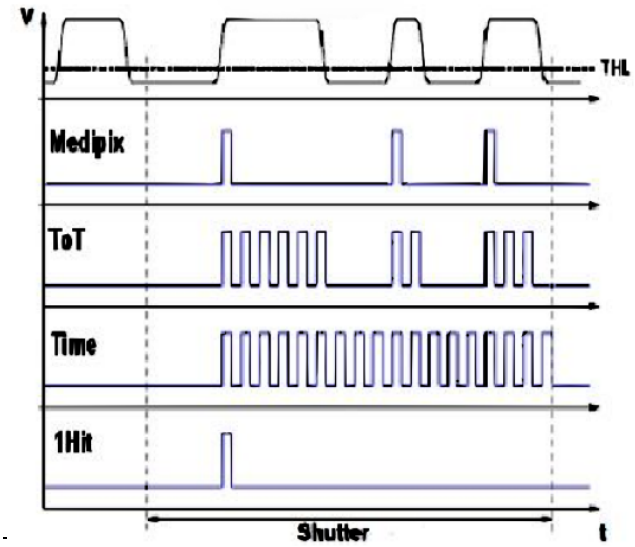

Figure 6: Modes of operation of Timepix detector.

As shown in Figure 6; the Timepix chip can operate in one of four modes:

- Medipix mode: the chip counts how many times during the open shutter the signal exceeds a certain threshold;
- Time-over-Threshold (ToT) mode: the chip measures for how long the signal stays above the threshold;
- Time-of-arrival (ToA) Mode: the chip measures time from the moment when the signal crosses the threshold until the shutter is closed;
- OneHit mode: the chip checks if the signal exceeds the threshold at least once during the open shutter.

To measure energy deposited in the sensor by a particle the ToT mode of the Timepix chip is used. In this mode, when the signal in a pixel crosses some threshold level THL the pixel counter starts counting pulses from the oscillator. It stops when the amplitude of the input signal falls below the threshold. The number of counted pulses depends on the amount of absorbed energy. The oscillator frequency can be set in the range of 10-2 MHz.

To determine the relationship between the value of ToT counts and the value of deposited energy E an energy calibration of the detector is required. The ToT-E relationship can be approximated by the following function (its general view is shown in Figure 7):

$$\boldsymbol{ToT(E) = a.E + b + \frac{c}{E-t}} \quad \textbf{(1)}$$

Its reverse function is the following:

$$E(ToT) = \frac{a.E + ToT - b + \sqrt{(b + a.t - ToT)^2 + 4.a.c}}{2.a} \quad \textbf{(2)}$$

Empirical formulas (1) and (2) were first proposed in (J. Jakubek et. al., 2008).

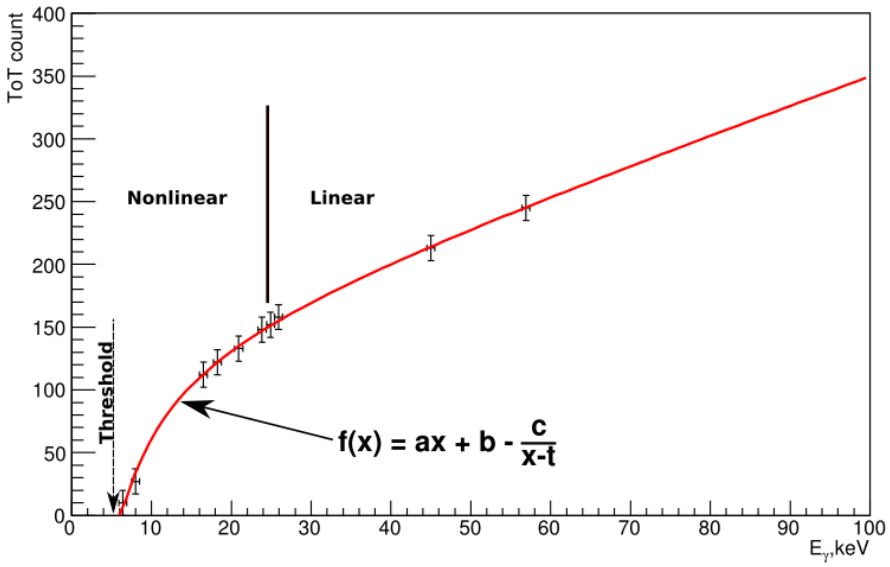

Figure 7: General shape of the calibration curve

Due to non-uniformity of the sensor material and the spread of parameters for individual channels of the Timepix readout chip, the coefficients a, b, c and t of the calibration curve will be different for different pixels. That means that procedure for the energy calibration must be done on per-pixel basis.

Calibration of the pixel detector is carried out in two stages. The first stage is the pixels threshold equalization. For this purpose the PIXET Pro software package is used. The threshold level THL is set the same for all pixels of the readout chip. But the electrical properties of each pixel are somewhat different due to technological features that lead to each pixel having its own noise level. Therefore, an additional corrective bias voltage is introduced into the amplifier channel of each pixel in order to equalize noise levels of all pixels at the set threshold level T HL.

The second step is the establishment of a one-to-one correspondence between the time length of the signal in ToT counts and the absorbed energy E. The procedure for obtaining E(ToT) dependence is called ToT-calibration. It can be done individually for each pixel (per-pixel calibration) and for the entire matrix as a whole (generalized calibration). Generally ToT-calibration comprises of the following steps:

- Measurements of X-ray spectra of known radioactive γ-sources and spectra of characteristic emission of selected materials in units ToT ;

- Identification of peaks in the recorded ToT-spectra with corresponding X-ray emission lines;
- Fitting of the peaks and constructing of a ToT (E) relation graph;
- Fitting of the obtained ToT (E) graph with the function (1) and calculation of the inverse relationship E(ToT) according to (2).

The spectra of characteristic emission of Ni, Cu, Zn, Zr, Mo, Rh, Cd, In, Sn and Ta were chosen as the benchmark spectra for the energy calibration (their K_α energy is listed in Table 1). This choice of foils allows to calibrate detectors in the energy range of [7,100] keV and takes into account the presence of two regions in the calibration curve. For the linear region above ~25 keV two reference energy points are needed while in the nonlinear region below 25 keV more control points are require to define the shape of the calibration curve with sufficient accuracy.

Foil (Element)	K_α in eV
Ni	7,478.15
Cu	8,047.78
Zn	8,638.86
Zr	15,775.1
Mo	17,479.34
Rh	20,216.1
Cd	23,173.6
In	24,209.7
Sn	25,271.3
Ta	57,532

Table 1 (A. Thompson et. al., 2009)

As mentioned above, the characteristic emission spectra used in the energy calibration were measured in the “reflection” geometry of the experimental layout (shown in Figure 8).

In this project, we used a hybrid Timepix detector with a GaAs:Cr sensor of 500 µm thickness. The bias voltage applied to the sensor was V bias = −500 V. To exclude the effects of temperature the sensor was thermally stabilized (at 20°C) with the use of a Peltier element with a heat output of up to 5 watts.

The microfocus X-ray tube SB 120-350 was used as the X-ray source. Recording of ToT spectra was done with the PIXET Pro software package. Data processing was carried out in the ROOT data analysis framework. By adjusting the position of the Timepix detector relative to the X-ray tube uniform illumination of the detector matrix was achieved. For all measurements the clock frequency of the Timepix pulse generator was set to f = 10 MHz, the threshold to THL = 220, the duration of the open shutter (time frame) was 1 ms.

Generalized calibration of Timepix detector

In this sub-section we illustrate the generalized calibration as part of our literature review only.

Initial data for the generalized calibration of Timepix detectors are the total TOT spectra obtained by summing statistics from all pixels.

This approach allows quickly calibrate the detector, since the time of data collection in this case is a few orders of magnitude smaller than the time of per-pixel calibration that needs considerable number of hits in every pixel. But the accuracy of generalized calibration is worse, because it does not take into account differences between the pixels caused by non-uniformity of the sensor material and quality of the detector assembly.

During the data collecting in order to eliminate the influence of the charge sharing effect only single-pixel events should be selected when absorbed photons create hits only in one pixel. The charge sharing appears when a single particle generates hits in several adjacent pixels. This is because the electron-hole cloud created in the sensor material by the absorbed or passing particle increases in size as it drifts to the electrodes, and eventually the charge can be shared by several pixels forming a cluster.

An important step of the calibration is the fitting of the reference spectral peaks to extract quantitative information about their positions and widths. The peaks in the spectra have the normal distribution shape, so they should be fitted using a Gaussian function with parameters properly chosen for each individual peak of characteristic emission.

Knowing the ToT values of the peak positions and the K_{α}, we can construct a graph of ToT(E). The fit to this graph should be performed in two steps. Firstly, in the energy range [25, 100] keV a straight line $a \cdot E+b$ should be used as the fitting function and the values of the parameters a and b should be determined. The second step is about fitting all the data points in the energy range [7, 100] keV with the function (1). As a result, all four parameters a, b, c, t should be determined.

Per-pixel calibration of Timepix detector

In this sub-section we illustrate the per-pixel calibration as part of our literature review and as a somehow detailed illustration of our project.

Since all pixels in a hybrid pixel detector give a somewhat different response to the passage of a particle with a certain energy, in order to have the best energy resolution of the detector the parameters of the calibration curve must be determined individually for each pixel. The basic idea of the calibration process is the same as in the generalized calibration, so only particular features of the per-pixel calibration and its automation will be discussed below.

In the per-pixel calibration ToT spectra obtained in each pixel are considered. Thus, a Timepix detector needs 65536 ToT spectra for a single energy point in the calibration curve to be processed and analyzed. To perform the fitting procedure on pixel spectra one needs to collect a considerable amount of statistics for each pixel. The majority of the measurements during the

per-pixel calibration are carried out until about 1000 hits per pixel have been collected. The following algorithm is implemented for automation of the per-pixel calibration procedure:

- Collecting of necessary statistics to build per-pixel ToT spectra of the characteristic emission of the selected element;
- Selecting in the spectra of each pixel a region containing a peak of known energy (the region is chosen individually for each spectrum);
- Fitting the selected region of the spectrum with a combined function.

Because the shape of the spectra from different elements varies from pixel to pixel, the limits on the fitting function parameters are selected for each ToT spectrum individually to ensure a better convergence of the fit. The range of the fitting function is defined as some neighborhood of the bin with the maximum value. The maximum likelihood method is used in the fitting, since it gives better results in the case of bins with low statistics. If a pixel is dead or is not working properly, it is neglected in further steps.

This procedure is conducted for all the selected target materials. Once a sufficient number of data points is collected, fits to the calibration curve are performed for each pixel individually similar to the case of the generalized calibration. As a result, one receives 65536 calibration curves relating the value of ToT measured by a pixel in the detector and the energy deposited in this pixel. And accordingly one has 4 parameters for each working pixel.

Experiment description

In this section we illustrate in some detail the set up of the experiment and the experimental instruments used. We also mentioned the software that we used for the data acquisition and data analysis.

Experimental Setup

1. The experimental setup consists of the following parts:
2. X-Ray tube.
3. Set of metal foils with different material for observation characteristic lines of metal.
4. Radioactive gamma source for the calibration verification.
5. Timepix detector with cooling system for semiconductor sensor (GaAs is very sensitive for changing the temperature).
6. HV power supply with an inbuilt ammeter.
7. PC for data acquisition.

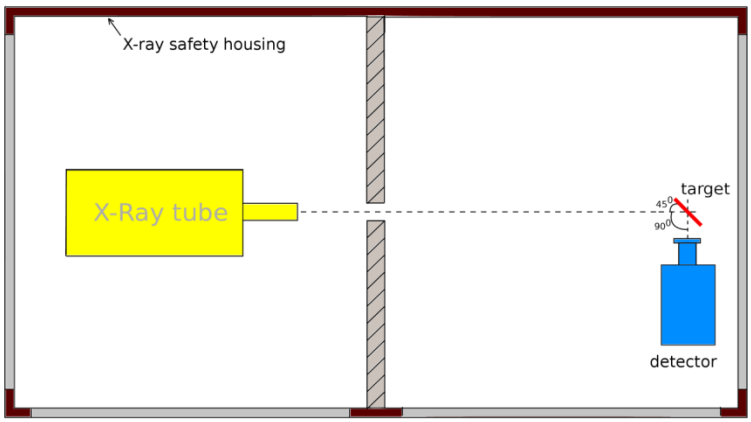

Figure 8: Experimental layout

X-Ray

Characteristic X-rays are emitted from elements when their electrons make transitions between the atomic energy levels. If an electron transitions from a level with energy E_i to one with energy E_j , the emitted X-ray has energy $E_X = E_i - E_j$. Because each element has a unique set of atomic energy levels, it emits a unique set of X-rays which are characteristic of this element.

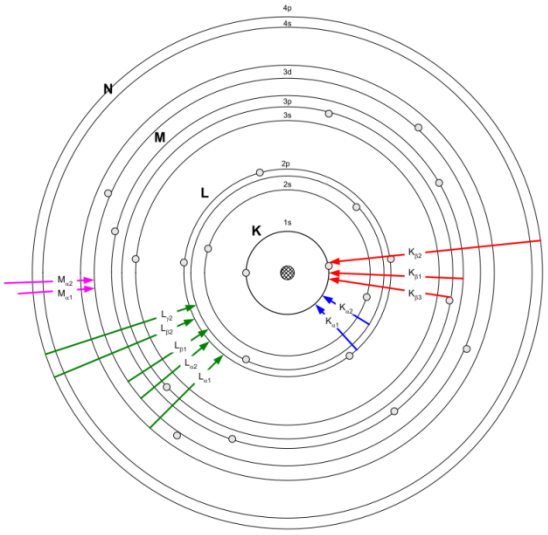

Figure 9: Representative sketch of an atom showing atomic energy levels.

Figure 9 is a sketch of an atom, showing the various atomic levels, designated K, L, M, N...etc. Each of these has additional sub-shells. The characteristic X-rays arise from transitions between these shells. The plot shows how the lines are named: A K X-ray arises from a transition to the K shell from an outer shell, and so on. A $K_{\alpha 1}$ X-ray, for example, arises when there is a vacancy in the K-shell and an electron drops from the M_3 shell to fill it. The atom then emits an X-ray with energy correspond to the difference: $E_{Xray} = E_K - E_{M3}$.

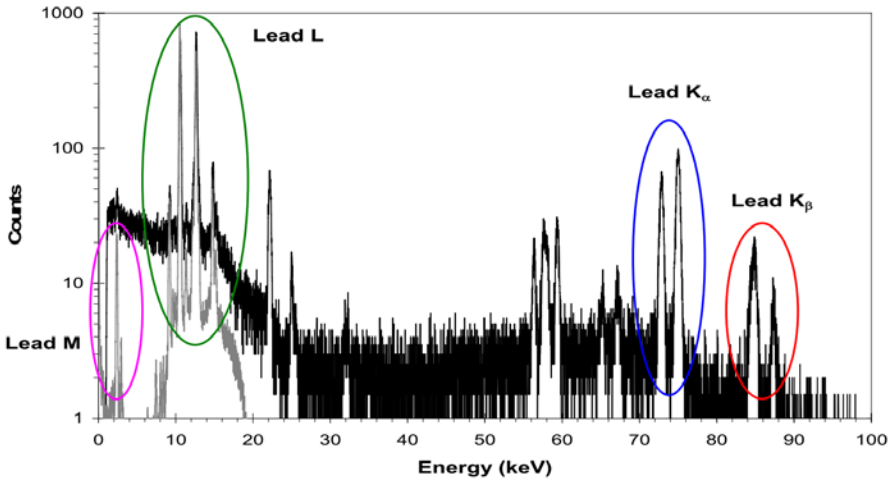

Figure 10: Pb characteristic X-Ray

Figure 10 shows measured characteristic X-rays emitted by lead. The K-shell electrons have a binding energy of 88.04 keV. The K_β lines correspond to transitions from the M and N shells, with energies of 85 and 87 keV. The K_α lines arise from transitions from the L shells, with energies of 72 and 75 keV. The L lines arise from transitions to the L shell, with energies of 10 to 15 keV. The M lines, arise from transitions to the outer M shells and have energies around 2.5 keV. (AMPTEK)

The x-ray source used was a micro-focus x-ray tubes which consist of features of x-ray units as follows:

- Small focal spot from 75/500 micron
- Adjustable voltage range from 60 to 120 kV
- Adjustable current range from 20 to 350 uA

The x-ray set is shown. SB-120-350 X-Ray unit has a wide range of applications, such as

gauging and inspection systems. (S.R.I)

Figure 11: SB 120-350

Data Acquisition Software

Threshold equalization of the pixels (Figure 13) & data were taken from the detector using PIXET Pro software(Figure 12). The PIXET Pro is multi-platform software developed in Widepix Company.

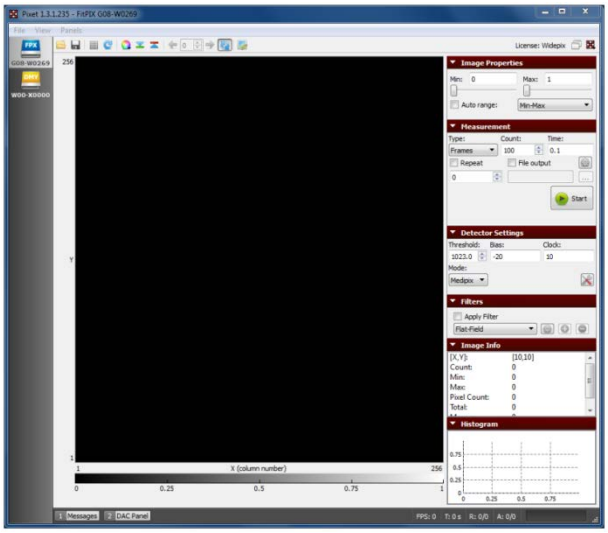

Figure 12: PIXET Pro Main Window.

It is a software package for Medipix family chips for acquisition control. It supports most of the available Medipix based devices (Medipix 2, Timepix, Medipix Quad, Timepix Quad, Widepix, Timepix3) and commonly used readout interfaces Minipix, FitPIX, ModuPIX, WidePIX, RasPIX, etc. PIXET Pro provides many tools for optimization of detector parameters, data processing, image corrections and scripting. PIXET Pro has an open architecture (not open source) supporting various types o f imaging detectors and related devices (e.g. control of positioning systems or X-ray tubes) and allowing integration of user plug-in modules prepared in C ++. Many of such plug-ins already exist s, e.g. Timepix chip equalization, calibration, beam-hardening correction, flat-field correction, particle track analysis, scripting in Python with syntax highlighting. PIXET Pro is written in C++ language and uses multi-platform. (WIDEPIX)

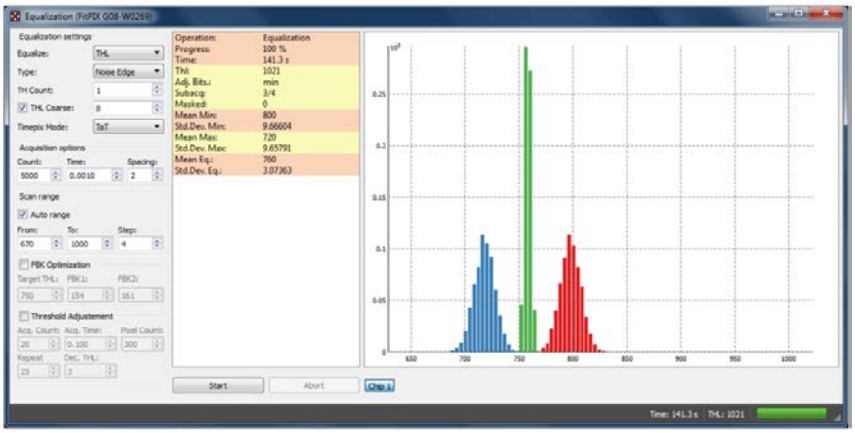

Figure 13: Pixel Threshold equalization using PIXET Pro.

Data Analysis Software

The data from the PIXET Pro software were analyzed by the ROOT software. ROOT is a modular scientific software framework. It provides all the functionalities needed to deal with big data processing, statistical analysis, visualization and storage. It is mainly written in C++ but well integrated with other languages such as Python and R. **Our codes (scripts) were written in C++.** (ROOT)

Figure 14: ROOT Data Analysis Framework

Results & validation

Our work was concentrated on the per-pixel calibration because all pixels in a hybrid pixel detector give a somewhat different response to the passage of a particle with a certain energy, which makes such method more effective than the generalized one (of course the trade off is the experiment's time).

The macros were developed for all the steps needed in the calibration; a step that was very educative and extremely time consuming.

We obtained the ToT spectra for each working pixel, and it was evident that for the first 9 foils around 20% of the pixels were not working well; either giving wrong signals or dead (for Thallium's experiment about 40% were not working well). ToT spectra for each single energy point in the calibration curve was processed and analyzed; we used 10 foils, thus we had 10 points (a sufficient number of energy points). Around 1000 count was recorded by each pixel before processing. Fitting for each working pixel's spectra was done in the region of the peak; we took 25 ToT units before it and 25 ToT units after it. The last procedure was done using iterative method for the fit with setting the center point for the fit as the peak of the previous one; 3 or 4 iterations were enough. Figure 15 shows the characteristic X-Ray spectrum for Cadmium foil for pixel (110,110), the Gaussian fitting is also shown and the result of the iterative fitting mentioned is evident, also the FWHM energy resolution of the detector is present. The remaining 9 foil's spectrum fitting are attached in the appendix of the report.

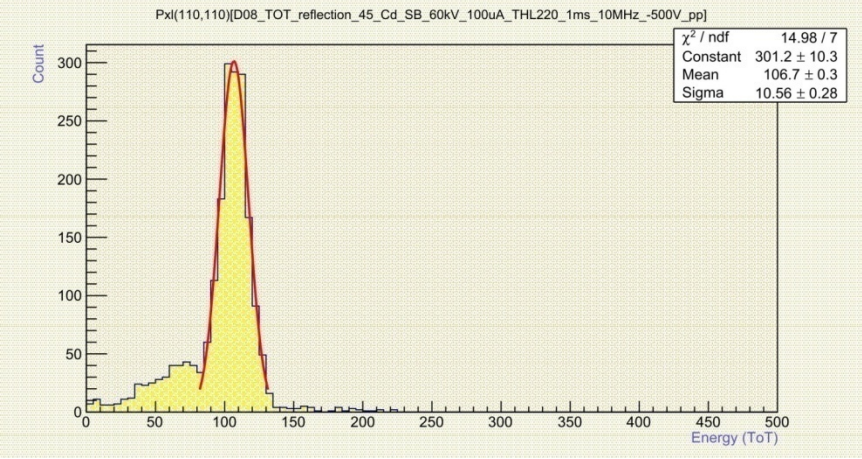

Figure 15: Fitted Characteristic X-Ray spectrum for Cadmium foil for pixel (110,110).

Fits to the calibration curve were performed for each working pixel individually, and the four parameters for each working pixel were obtained. Figure 16 shows the final energy points fitted first for energy beyond 25 KeV with linear function, then parameters a and b were used to fit the complete range with the complete empirical equation (1), all of that done for pixel (110,110). The resulting parameters for such pixel were: a=2.92601, b= 41.2049, c=77.0121 and

t=4.80152. Such procedure is done for all working pixels and for each one the four parameters were obtained and saved.

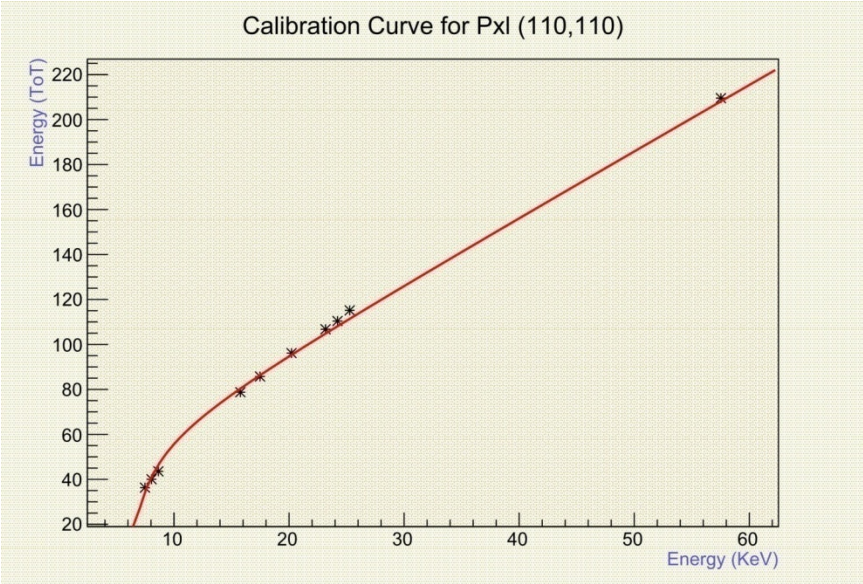

Figure 16: Fitted calibration curve for pixel (110,110)

To validate our results, we used a gamma emitting radioactive source: Am-241. We averaged each parameter for all the pixels, and the resulting averaged parameters were as follows: a=2.90578, b=37.1093, c=73.7067 and t=4.72846. Figure 17 shows the fitted (the same iterative method mentioned above for the fitting range was used) gamma spectrum of the Americium source, the Gaussian Mean (ToT energy peak) was equal 210.045, when using the 4 parameters and converting it to KeV energy it becomes 59.9737; a value that is very close to the 59.6 KeV (Am-241 peak)!

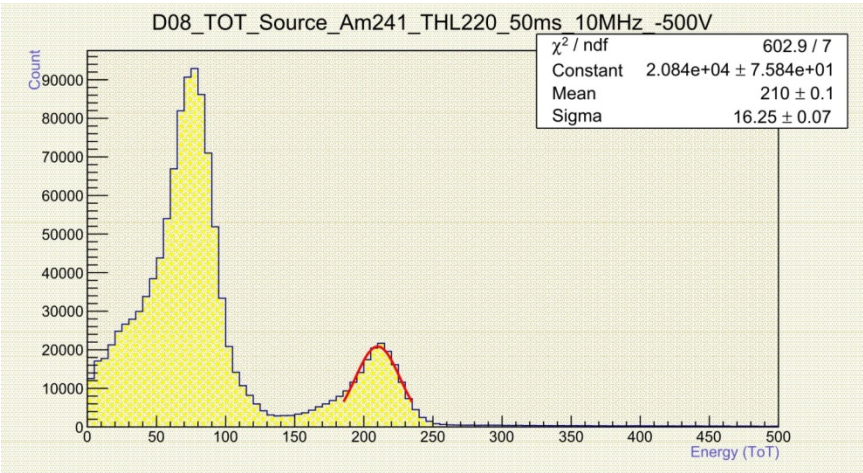

Figure 17: Fitted gamma spectrum for Am-241.

Discussion & recommendation for future students

The verification experiment shows that the calibration was successful for high energy particles (~ 60 KeV).

The project was mainly for practice and gaining experience in the field of experimental particle physics and computational methods in physics, it was not aimed at inventing a new technique or tool! From such practice I have gained a satisfactory knowledge of semiconductor pixel detectors (especially sensors on Timepix chip), energy calibration, C++, OOP, and data analysis using ROOT. I would strongly recommend future students to have a powerful practical experience in C++ (or any other programming language) and at least basic experience in ROOT (or any other data analysis software using your language of expertise). Of course C++/Python and ROOT are preferred as ROOT is the main data analysis program used in HEP. I also recommend that you have fair background knowledge of Timepix detector, especially in its operational modes and performance; you can find good resources on the internet and you can always refer to your supervisors.

Further steps

It is preferred to perform a convolution/Monte Carlo simulation of the Timepix detector's reading so you choose the right energy peak, as it is not precisely the K-Alpha peak due to the energy resolution limitations of the detector. Also it would be better if more verification experiments were made. Finally, checking the validation of the energy calibration with beta-rays (after validation of the energy calibration with photons) using a beta emitting source or a magnetic electron separator would be a good step.

Acknowledgment

This practice would not have given me such satisfactory knowledge and experience without the strong guidance of Petr Smolyanskiy, I would like to thank him for his sincere effort. The time that Danila Kozhevnikov spent with me discussing ideas for experiments and performing an experiment with MARS CT Scan was very beneficial for me and is much appreciated. I would like to thank Dr Georgy Shelkov as well. The guidance of Dr Said Abdul Shakour was very helpful and his discussions were enlightening. Also I would like to thank Prof *Alexey* Zhemchugov for his continuous support and for a 3-lecture-series on GEANT4 that he gave and Prof Alexey Guskov for a general lecture on ROOT that he gave. I shall say that working in the Colliding Beam Physics Department, DLNP, JINR is a very satisfactory experience for me due to the helping and cooperative environment of the department. Finally, I feel all the gratitude for my friends, Eslam Ramadan and Omar Barakat, for their support concerning C++.

Bibliography

1. A. Thompson et. al. (2009). *X-Ray Data Booklet.* California: Lawrence Berkeley National Laboratory.
2. AMPTEK. (n.d.). *What is XRF?* Retrieved 10 25, 2015, from AMPTEK: Products for your imagination: http://www.amptek.com/xrf/
3. J. Jakubek et. al. (2008). Pixel detectors for imaging with heavy charged particles. *Nuclear Instruments and Methods in Physics Research* , 155-158.
4. Knoll, G. F. (2010). *Radiation Detection and Measurments* (Fourth ed.). New York: John Wiley & Sons, Inc.
5. Llopart, Ballabriga, Campbell, Tlustos & Wong. (2007, August 14). Timepix, a 65k programmable pixel readout chip for arrival time, energy and/or photon counting measurements. *Nuclear Instruments and Methods in Physics Research* , 485–494.
6. ROOT. (n.d.). *ROOT: Data Analysis Framework*. Retrieved 10 20, 2015, from ROOT: https://root.cern.ch/
7. Rossi, Fischer, Rohe, Wermes. (2005). *Pixel Detectors: From Fundamentals to Applications.* Geneva: Springer.
8. S.R.I. (n.d.). *SRI Products.* Retrieved 10 20, 2015, from SourceRay Inc.: http://www.sourceray.com/
9. WIDEPIX. (n.d.). *PIXET Pro users manual.* Retrieved 10 20, 2015, from WIDEPIX s.r.o: www.widepix.cz

Appendix

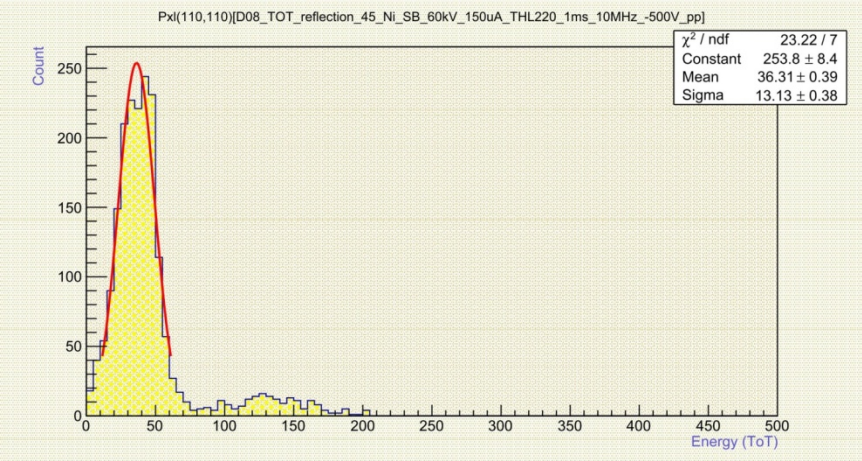

Figure 18: Characteristic X-Ray spectrum for Nickel foil for pixel (110,110).

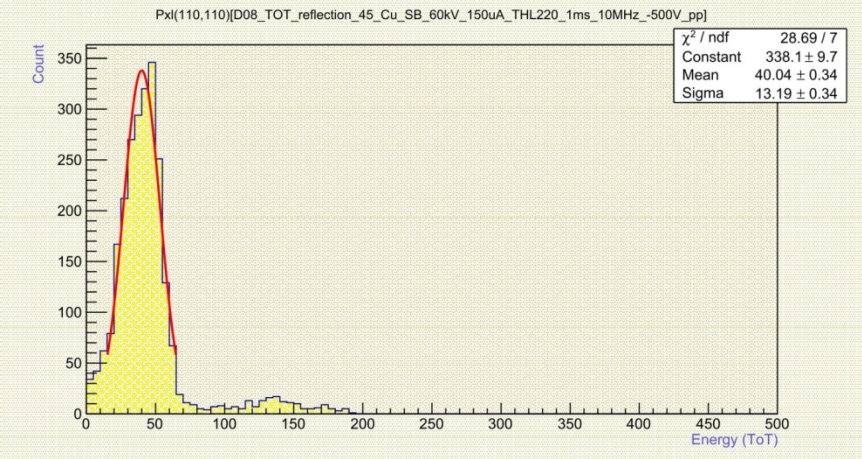

Figure 19: Characteristic X-Ray spectrum for Copper foil for pixel (110,110).

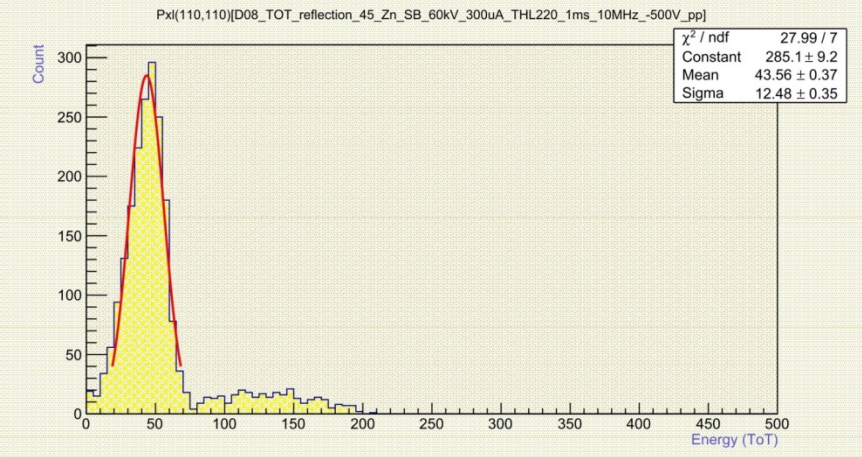

Figure 20: Characteristic X-Ray spectrum for Zinc foil for pixel (110,110).

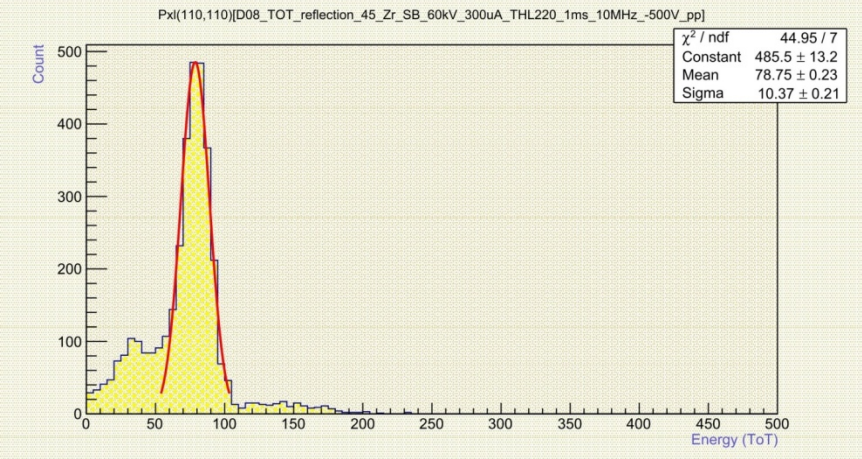

Figure 21: Characteristic X-Ray spectrum for Zirconium foil for pixel (110,110).

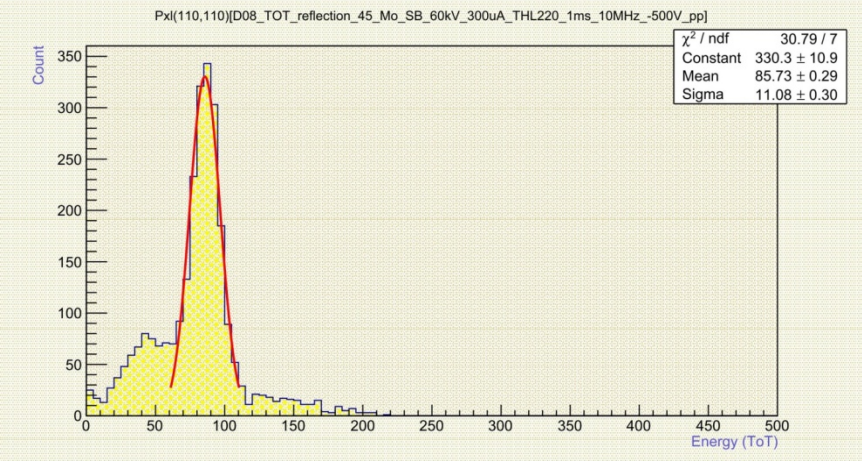

Figure 22: Characteristic X-Ray spectrum for Molybdenum foil for pixel (110,110).

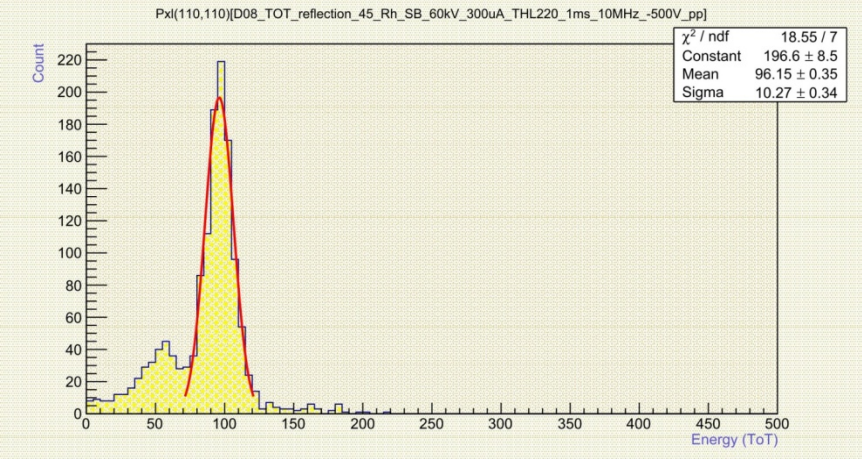

Figure 23: Characteristic X-Ray spectrum for Rhodium foil for pixel (110,110).

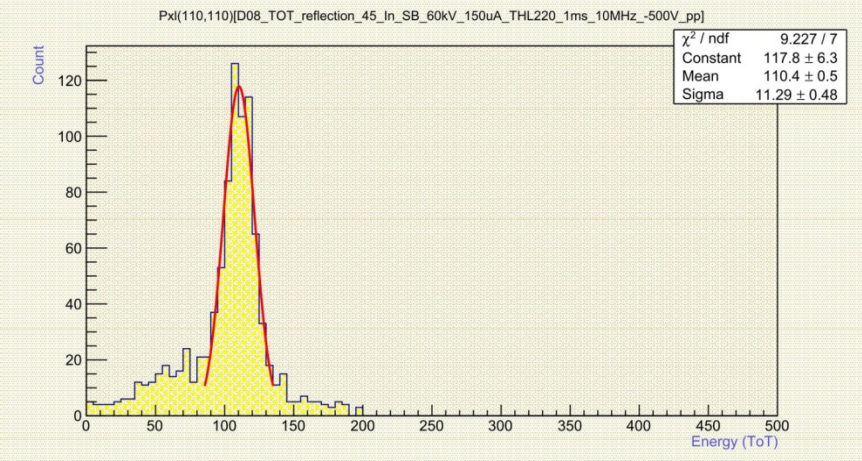

Figure 24: Characteristic X-Ray spectrum for Indium foil for pixel (110,110).

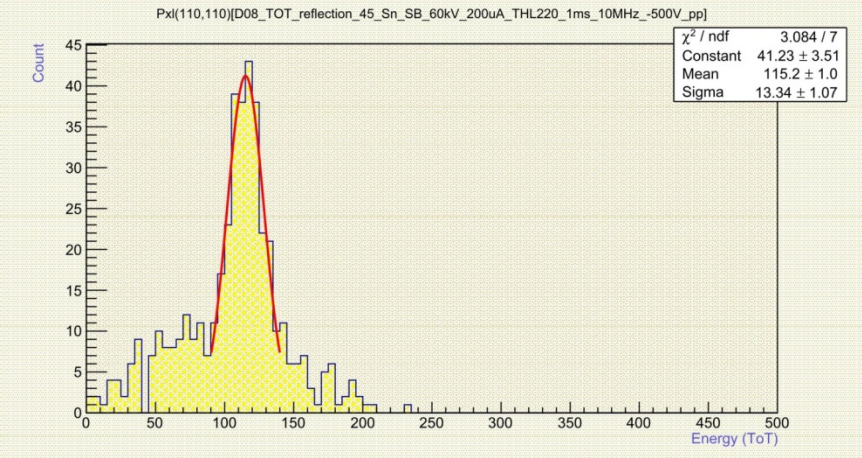

Figure 25: Characteristic X-Ray spectrum for Tin foil for pixel (110,110).

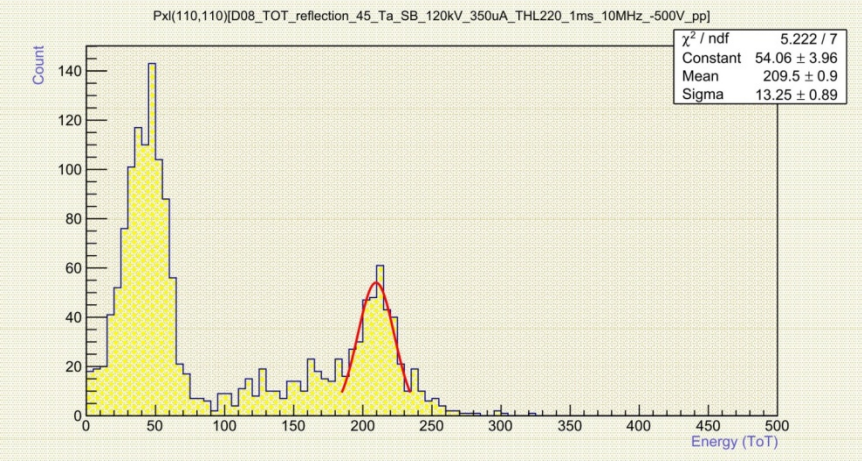

Figure 26: Characteristic X-Ray spectrum for Thallium foil for pixel (110,110).